Cellular & Molecular Biology
Cell. Mol. Biol. 2014; 60 (4): 30-36
Published online November 25, 2014 (http://www.cellmolbiol.com)
Received on July 10, 2014, Accepted on November 11, 2014.
doi : 10.14715/cmb/2014.60.4.5

SiRNA-mediated knockdown against NUF2 suppresses tumor growth and induces cell apoptosis in human glioma cells

S-K. Huang[1], J-X. Qian[2], B-Q. Yuan[1], Y-Y. Lin[1], Z-X. Ye[1] and S-S. Huang[3]✉

[1] Department of Neurosurgery, The 476th Hospital of Fuzhou General Hospital, Fuzhou 350025, Fujian,China
[2] Department of Medical Oncology, Changzheng Hospital, Shanghai, 200070,China.
[3] Department of Neurosurgery, Fujian Provincial Hospital, Fuzhou, 350025, Fujian, China.

Corresponding author: Shao-song Huang. Department of Neurosurgery, Fujian Provincial Hospital, Fuzhou, 350025, Fujian, China. Email: huangshso@163.com

Abstract

Glioma is one of the most commonly malignant brain tumors. Current therapies for glioma have failed to achieve satisfactory results, which necessitates the development of novel molecular therapies. In the current study, we aimed to investigate the role of NUF2 (Ndc80 kinetochore complex component) in glioma cell growth and assessed the possible mechanisms underlying NUF2-mediated glioma development. The lentivirus-based short hairpin RNA-expressing vectors were constructed and transfected into U87 and U251 cells. Real time PCR and western blot were performed for expression level determination. Annexin V-FITC/PI flow cytometric assay was conducted to determine apoptotic cell proportions. Cell viability *in vitro* and tumorgenic ability *in vivo* were assessed by MTT assay and a nude mouse xenograft, respectively. We found that NUF2 was overexpressed in glioma tissues and differentially expressed in a series of glioma cell lines. Depletion of NUF2 by short-hairpin RNA inhibited cell growth *in vitro* and *in vivo*. Furthermore, NUF2 depletion-induced growth inhibition was associated with cell cycle arrest and apoptosis. Aberrant expressions of cell cycle regulators and apoptosis-related proteins further confirmed that NUF2 depletion induced cell cycle arrest and apoptosis. In all, our results indicate that siRNA-mediated knockdown against NUF2 may be a promising therapeutic method for the treatment of glioma.

Key words: NUF2, siRNA, tumorigenesis, glioma.

Introduction

Cancer is now globally recognized as one of the leading causes of death (1, 2), claiming over 11 million lives annually with a rising rate of incidence, which is estimated to rise to 16 million by 2020 (3, 4). Approximately 2% of cancer patients are suffering from gliomas, which are considered the most common primary malignant tumors from the central nervous system (CNS) (5). Glioma is now clasffied as astrocytomas (Grade I–IV), oligodendrogliomas (Grade II and III) or mixed oligoastrocytomas (Grade II and III) (6). Featured by high morbidity and mortality, glioma is now one of the greatest threats to human health, with only 15 months median overall survival period for the most aggressive grade IV astrocytoma (7). Currently, treatments of human malignant glioma consist mainly of surgical resection, adjuvant radiation and chemotherapy (8). Despite newly arising therapeutic strategies, current therapies have failed to achieve satisfactory results (8).

Recent discoveries of molecule-targeted therapy have greatly advanced our understanding of disease onset. Among which, the NDC80/NUF2 complex proteins are frequently implicated in triggering tumorigenesis (9). NDC80/NUF2 complex consists of four proteins Spc24, Spc25, NUF2, and Hec1/NDC80. Members of the NDC80/NUF2 complex have been shown to be critically involved in the stable kinetochore-microtubule attachments and transchromosome alignment in mitosis (10-12). In Hela cells, it was shown that depletion of NUF2 by specific RNAi resulted in a strong block of prometaphase in cell cycle (11). Likewise, knockdown of Hec1 (human NDC80 homolog) by specific RNA interference was causable for blocking Mad1 and Mad2 from binding to kinetochores (12).

Dysregulation of NDC80/NUF2 complex has been implicated in a wide range of human cancer developments. In non-small cell lung cancers (NSCLC), overexpression of NUF2 and Hec1 was reported to be associated with poor prognosis, and siRNA-mediated knockdown against NUF2 or Hec1 has been found to inhibit cell proliferation and induction of apoptosis in NSCLC, ovarian cancer and cervical cancer (13, 14). Recently, it was also observed that both NUF2 and Hec1 were highly expressed in colorectal and gastric cancers. Depletion of NUF2 and Hec1 by specific siRNAs suppressed cell proliferation and induced apoptosis in colorectal and gastric cancer cells (15). In view of all these observations, it could be hypothesized that NUF2 might be critically involved in human cancer developments. However, the role of NUF2 in human glioma remains unclear. In addition, crosstalk between microtubule attachment complexes is critical for accurate chromosome segregation (9), we therefore hypothesized that regulation of NUF2 expression might also be central to glioma cell growth.

To this end, we first investigated the expression profile of NUF2 in glioma tissues and a set of glioma cell lines. Thereafter we employed short-hairpin RNA interference (shRNA) technology to stably deplete NUF2 expression in glioma cell lines. Cell viability *in vitro* and tumorgenic ability *in vivo* were assessed. Cell cycle

and apoptosis analysis were also included in the present study.

Materials and methods

Cell lines and cell culture

293 cell line and five glioma cell lines SHG-44, U87MG, A172, U87 and U251 were all purchased from Cell Bank of Chinese Academy of Sciences (Shanghai, China). All cells were maintained in DMEM (Gibco, MD, USA) containing 10% FBS (Gibco) at 37°C in a 5% CO_2 humidity-controlled incubator.

Reagents

Rabbit polyclonal NUF2 antibody was purchased from Abcam (Hongkong, China). Primary antibodies against Bcl-2, Bad, Cyclin B1, Cdc25A and β-actin were commercially obtained from Santa Cruz (Santa Cruz, CA. USA). Specific short-hairpin RNA targeting NUF2 (shNUF2) was purchased from Santa Cruz (Santa Cruz, CA, USA). For control, a negative control shRNA (shCon) was also used. Cell counting kit-8 (cck-8) was purchased from Dojindo (Japan).

RNA extraction and quantitative real-time PCR (qRT-PCR)

Total RNA was extracted by using Trizol reagent (Invitrogen, USA) according to the manufacturer's instructions. RNA sample was then subjected to quality assessment by visualizing 28S and 18S rRNA bands in a 1.5% gel electrophoresis and was subsequently quantified by Nanodrop 1000 spectrophotometer (Thermo Fisher Scientific, USA). cDNA was generated by using Superscript VILO™ cDNA Synthesis kits (Invitrogen, USA) according to the manufacturer's protocols. Quantitative PCR (qPCR) was performed with the Quanti-Tect SYBR Green PCR kit (Qiagen, Shanghai, China). Primers used for NUF2 were as follows: Forward: 5'-TACCATTCAGCAATTTAGTTACT-3'; Reverse: 5' TAGAATATCAGCAGTCTCAAAG-3' Primers used for internal control gene β-actin were Forward: 5' CAGAGCCTCGCCTTTGCCGA-3' Reverse: 5'-AC-GCCCTGGTGCCTGGGGCG-3'. PCR cycle conditions were set as 95°C for 30 s, and 39 cycles of 95°C for 5 s and 60°C for 34 s. Amplification specificity was evaluated by melting curve analysis. Data were obtained from three independent experiments.

Western blot analysis

24h post culture, cell lysate was harvested using RIPA buffer. After centrifugation at 4°C for 15 min (12,000 g), the supernatant was collected. Protein concentration was determined using a BCA kit (Pierce, Rockford, IL). Equal amounts of extract (30ng) were loaded to each lane in a 12% SDS-PAGE and transferred to polyvinylidene difluoride (PVDF) membranes (Bio-Rad, Hercules, CA). After antigen blocking in TBST supplemented with 5% fat-free milk for 1h, the membranes were blotted with corresponding primary antibodies overnight at 4°C. Membranes were then incubated with secondary antibodies for 1h at room temperature and processed for chemiluminescent detection with an ECL system (Pierce, Rockford, IL).

Cell apoptosis assay

To assess cell apoptosis, the annexin V-FITC/ propidium iodide (PI) flow cytometric assay was conducted in order to determine the proportion of apoptotic cells in distinct groups. Briefly, harvested cells were suspended in the binding buffer at a concentration of 2×10^6 cells/ml. Cells were then incubated with annexin V-FITC for 20min, followed by incubation with PI for 6min in the darkness. At least 1×10^4 stained cells from each group were analyzed by flow cytometer. Results were then analyzed with CELL Quest software (BD Biosciences).

Fluorescence-activated cell sorting analysis (FACS)

To determine cell cycle distribution of Lv-shNUF2- or Lv-shCon-infected cells, flow cytometry assay was performed following PI staining. In brief, cells were collected 96h after infection with lentivirus expressing GFP- shNUF2 (Lv-shNUF2) or GFP only (Lv-shCon) and subjected to seeding in 6-well plates (3×10^5 cells per well) for attachment overnight. PBS-washed Cells were then suspended and fixed in 0.5 ml of 70% cold alcohol and kept at 4°C for 30 min. After fixation, 100 mg/ml of DNase-free RNase (MBI Fermentas) and 50 mg/ml of PI (Sigma-Aldrich) were added to cell suspension before cells were proceeding for incubation at 37°C for 30 min. The suspension was filtered through a 50-mm nylon mesh, and a total of 1×10^4 stained cells were analyzed by a flow cytometer (FACS Cali-bur, BD Biosciences).

Cell viability assay

The MTT assay was employed to examine cell viability. U87 and U251 cells that infected with Lv-shNUF2 or Lv-shCon were seeded on a 96-well plate at a density of 1×10^4 cells/well to reach a confluence of approximately 70%. Cells were then washed with PBS, and 10μL of MTT (0.5 mg/ml diluted by culture medium) were added to each well, followed by 3h incubation at 37 °C in the dark. The absorbance at 450nm (A450) was then measured with a microplate reader (Multiscan MK3, Thermo).

Nude mouse xenografts

To reveal effects of NUF2 depletion on glioma growth *in vivo*, nude mouse xenografts were conducted as described previously (18). Specific pathogen-free eight-week-old female BALB/C-nu/nu mice were purchased from the Cancer Research Center of Shanghai and maintained under specific pathogen-free conditions. When mice were adapted to the environment, each mouse was subcutaneously inoculated with 200μl of medium that contains 2×10^7 shNUF2-transfected U87 cells or U251 cells in the forelimb (shNUF2 group). For control, mice were injected with mock-injected cells (shCon group). Tumor size was measured in two dimensions with calipers twice a week, up to 30 days after injection. Tumor volume (v) was calculated according to the formula $V=L\times W^2/2$ (L represents length while W represents width). Procedures were approved by the Animal Care and Use Committee. All efforts were made to minimize suffering.

Statistical analysis

Data were analyzed with SPSS 15.0 software and

presented as mean ± standard deviation (SD). Significance was determined by using paired t test. P<0.05 were considered significantly different.

Results

NUF2 is highly expressed in glioma tissues

Previously, microarray data showed that average mRNA level of NUF2 in ten cases of glioma was 28-fold higher than that in the paired adjacent tissues. To confirm our observation, we performed qRT-PCR analysis of NUF2 mRNA level in the ten cases of glioma and their paired adjacent tissues. It was shown that mRNA level of NUF2 in the non-cancer tissues was only 2.5, whereas it was as high as 12 in the glioma tissues (Figure 1, ***P*=0.006). These data suggest that NUF2 is overexpressed in glioma tissues.

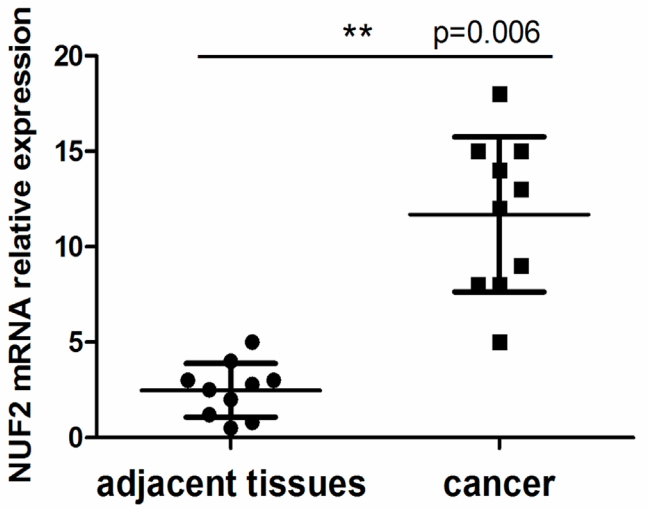

Figure 1. NUF2 is highly expressed in glioma tissues. mRNA level of NUF2 in the non-cancer tissues was only 2.5, whereas it was as high as 12 in the glioma tissues. ***P*=0.006

Expression profile of NUF2 in a set of cell lines

To reveal the expression profile of NUF2 in human glioma cell lines, frequently used glioma cell lines such as U251, U87, SHG-44, U87MG and A172 were cultured here. 293 cells were also used as control. As shown in Figure 2A, NUF2 was differentially expressed in these cell lines. Relative quantification of protein expression levels further revealed that U251 and U87 cell lines had highest NUF2 protein expression, while SHG-44, U87MG and A172 had moderate NUF2 expression. 293 cells, as expected, had lowest NUF2 expression (Figure 2B). Consistently, mRNA of NUF2 showed the highest levels in U251 cells and U87 cells (Figure 2C). These observations suggest that NUF2 is differentially expressed in glioma cells.

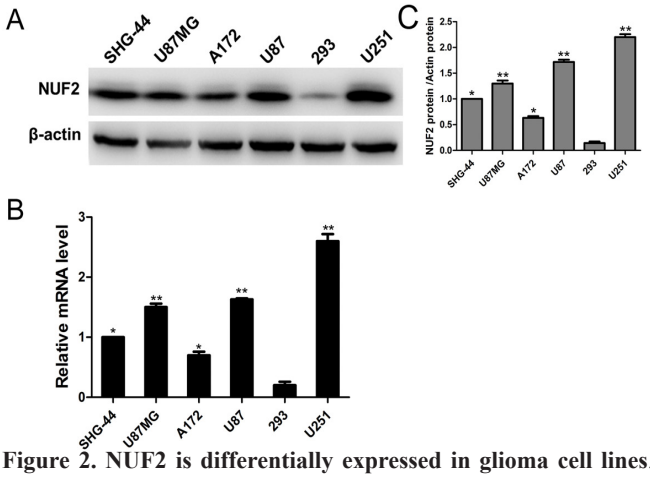

Figure 2. NUF2 is differentially expressed in glioma cell lines. (**A**) Western blot analysis showed that protein levels of NUF2 were different in distinct glioma cell lines. (**B**) Relative quantification of protein levels showed that U251 and U87 cell lines had highest NUF2 expression, while SHG-44, U87MG and A172 had moderate NUF2 expression. Lysates from 293 cells were loaded as control and shown to have lowest NUF2 expression. (C) qRT-PCR analysis further showed that U251 cells and U87 cells exhibited the highest mRNA level of NUF2. *, p<0.05 , **, p<0.01.

NUF2 was successfully depleted by lentivirus-delivered short-hairpin RNA

To study the role of NUF2 in glioma cell growth, we employed shRNA technology to stably deplete expressions of NUF2 in U87 cells and U251 cells that had the highest NUF2 expression levels. Infection efficiency was confirmed as judged by the bright vision and GFP expression under the fluorescent microscope (Figure 3A). Total RNAs from U87 and U251 were then extracted and subjected to qRT-PCR analysis. Figure 3B showed that infection with Lv-shNUF2 significantly

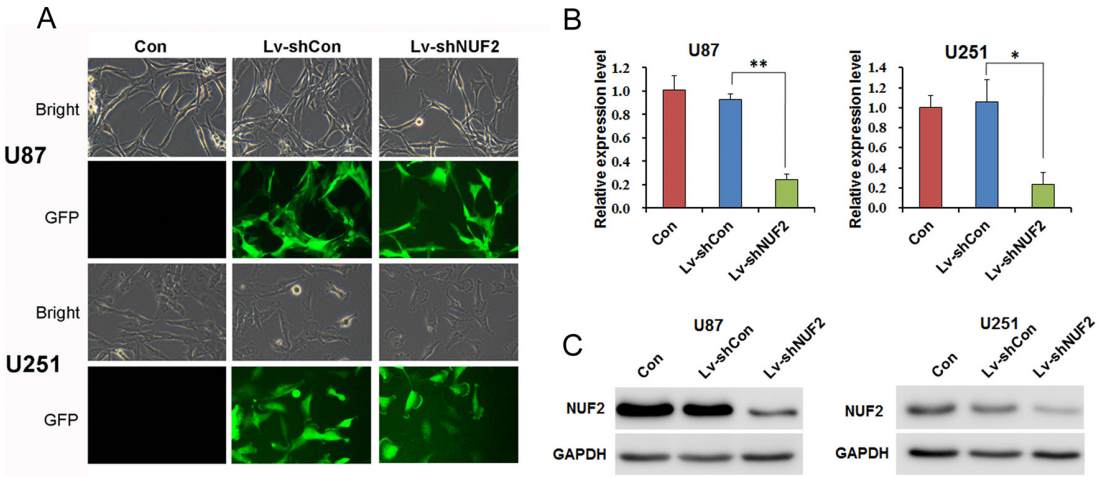

Figure 3. Lentivirus stably expressing shRNA against NUF2 was successfully constructed. (**A**) Infection was observed to be efficient 96h post infection. Over 80% U87 and U521 cells presented to be GFP positive in both Lv-shCon and Lv-sh NUF2 groups. (**B**) qRT-PCR analysis verified that mRNA level of NUF2 was successfully decreased after infection of Lv-shNUF2 in both U87 and U521 cells. (**C**) Western blot analysis validated that protein level of NUF2 was knocked down after infection with Lv-shNUF2. *, p<0.05 , **, p<0.01.

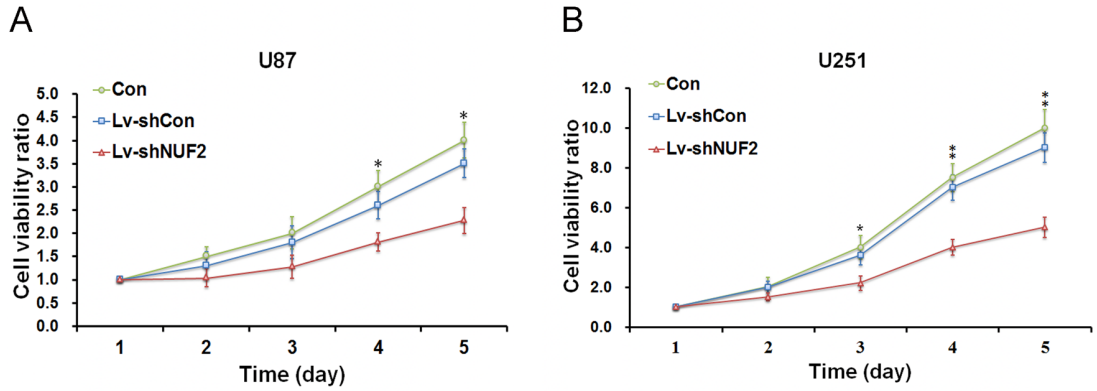

Figure 4. NUF2 depletion inhibits U87 and U251 cells proliferation. MTT assay was performed. Results showed that cell numbers were significantly decreased in U87 (**A**) and U251 cells (**B**) when compared with control group on day 4 and day 5.*,P<0.05, **, p<0.01.

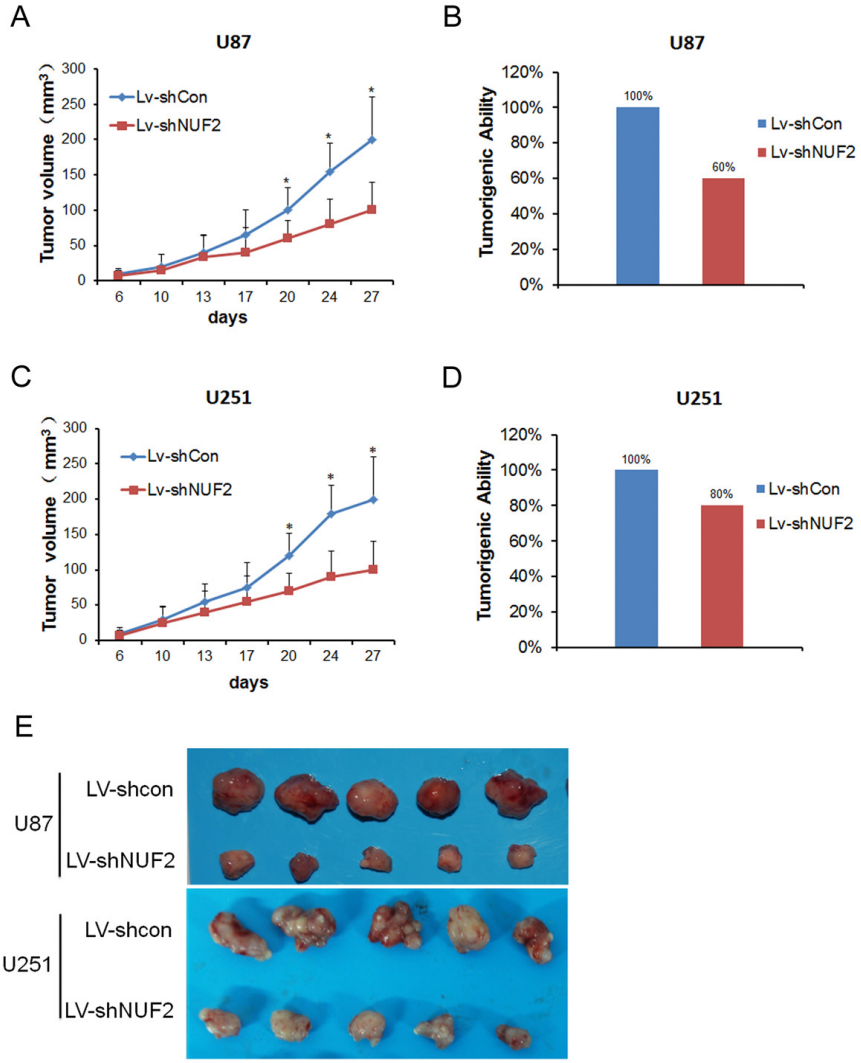

Figure 5. NUF2 depletion inhibits tumor growth in a mice model of glioma. (**A**) In U87 cells, tumor size was significantly smaller since day 17. Tumor size was even approximately 50% of that in the Lv-shCon group. (**B**) Moreover, while all mice in Lv-shCon developed to bear glioma, only 60% mice in Lv-shNUF2 group developed glioma. (**C**) In U251 cells, tumor volume became to be limited since day 13, and on day 27, it was only half of that in the Lv-shCon group. (**D**) Only 80% mice that infected with Lv-shNUF2 developed glioma in U251 cells. (**E**) images of dissected tumors in each group were presented. *P<0.05

decreased mRNA levels of NUF2 in both U87 and U251 cells, while shCon caused no significant differences to control group (Figure 3B). Furthermore, western blot analysis revealed that protein levels of NUF2 in both U87 and U251 cells were also significantly ablated (Figure 3C). Taken together, it could be concluded that construction of lentivirus stably expressing shRNA against NUF2 in U87 and U251 cells was successful.

Depletion of NUF2 significantly inhibits cell proliferation in U87 and U251 cells

We then performed MTT assay to assess the effects of NUF2 depletion on cell proliferation. In U87 cells, we found that cells infected with Lv-shNUF2 exhibited slower proliferative ability since day 2. On day 5, cell proliferation was even slowed down by 50% as compared with control U87 cells (Figure 4A). Similarly, cell proliferation was significantly decreased since day

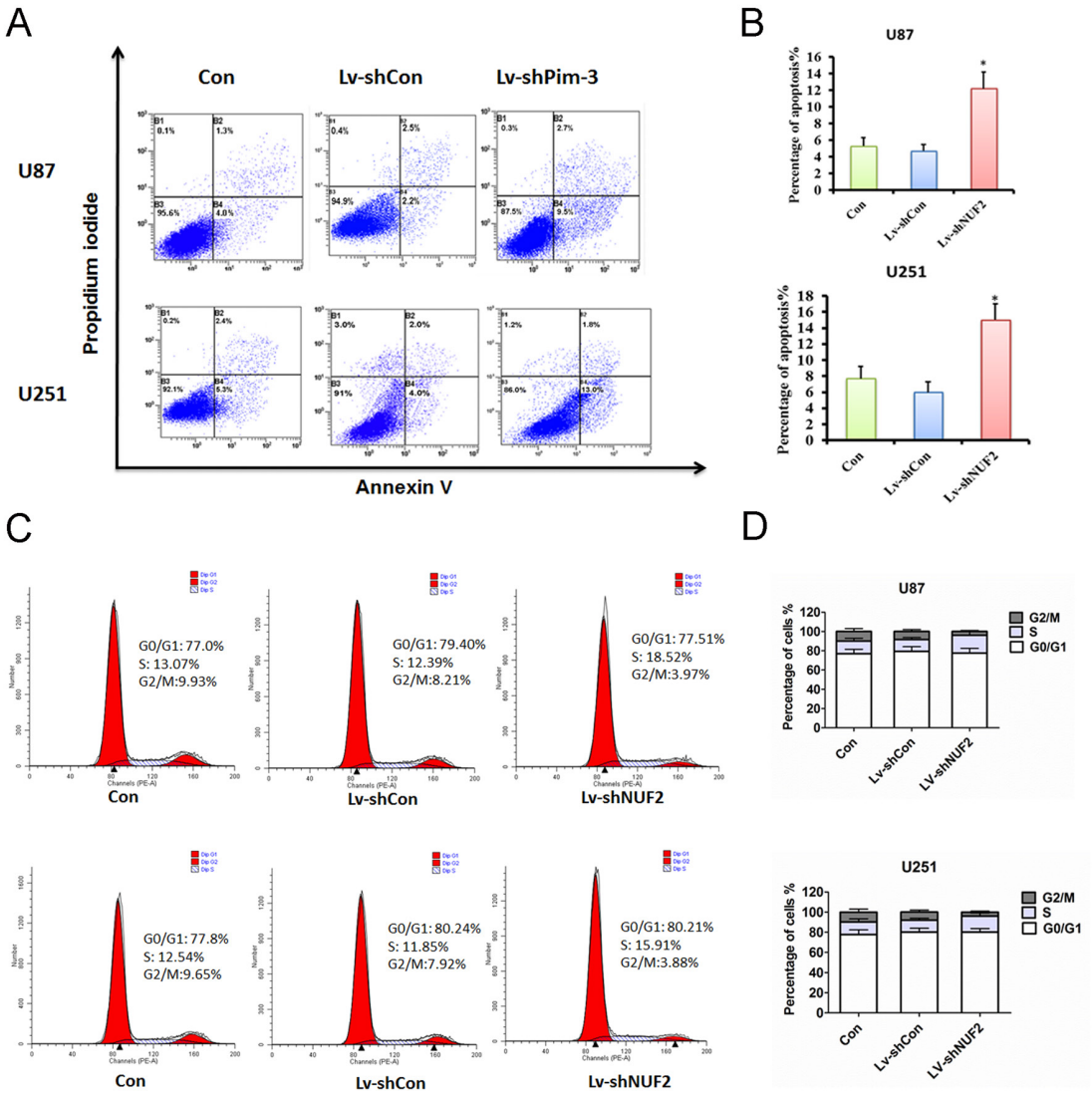

Figure 6. Depletion of NUF2 induces cell apoptosis and affects G2/M phase in cell cycle. (**A**) Annexin-V/PI assay was performed to detect apoptotic cells. (**B**) it was shown that only 5% of cells were apoptotic in control U87 cells. However, nearly 12% U87 cells infected with Lv-sh-NUF2 were shown apoptotic. Similarly, only 8% control U251 cells were apoptotic. However, 14% U251 cells that infected with Lv-shNUF2 died of apoptosis. (**C**) Cell proportion of cell cycle phases was also determined. (**D**) Cell proportion in G2/M phase was significantly changed in both Lv-shNUF2-infected U87 and U251 cells.

3 in U251 cells. On day 5, cell numbers were further decreased by 60% (Figure 4B). These data suggest that depletion of NUF2 in U87 and U251 cells could inhibit cell growth.

Depletion of NUF2 significantly inhibits tumor growth in a mice model of glioma

To further assess effects of NUF2 depletion on tumor growth *in vivo*, we first set up a mice model bearing glioma. Tumor volume was periodically measured and calculated. In U87 cells, tumor size was significantly smaller since day 17. Tumor size was even approximately 50% of that in the Lv-shCon group (Figure 5A). Moreover, while all mice in Lv-shCon developed glioma, only 60% mice in Lv-shNUF2 group developed glioma (Figure 5B). Likewise, in U251 cells tumor volume became to be limited since day 13, and on day 27, it was only half of that in the Lv-shCon group (Figure 5C). Only 80% tumorigenic rate explained the smaller tumor size in Lv-shNUF2 group (Figure 5D). Photographs of 5 representative tumors from each group are also shown (Figure 5E). Altogether, tumor growth is significantly inhibited after NUF2 is depleted from U87 and U251 cells.

Depletion of NUF2 induces cell apoptosis and affects G2/M phase in cell cycle

Furthermore, we performed annexin-V/PI assay to detect apoptotic cells (Figure 6A). We found that only 5% of cells were apoptotic in control U87 cells. However, nearly 12% U87 cells infected with Lv-shNUF2 were shown apoptotic. Similarly, only 8% control U251 cells were apoptotic. However, 14% U251 cells that infected with Lv-shNUF2 died of apoptosis (Figure 6B). These results indicated that cell apoptosis was induced by NUF2 depletion. In addition, we detected cell proportion of cell cycle phases (Figure 6C). As showed in Figure 6D, we found significant changes in G2/M phase in both Lv-shNUF2-infected U87 and U251 cells, indicating that depletion of NUF2 interrupted cell cycle, especially G2/M phase.

Depletion of NUF2 affects apoptosis-related and G2/M phase-related protein expressions

To further confirm that depletion of NUF2 could induce cell apoptosis and affect G2/M phase, we selected several proteins which are closely linked with apoptosis (Bcl-2 and Bad), or associated with G2/M phase (Cyclin B1 and Cdc25A). Bcl-2 is an apoptosis inhibitor, while

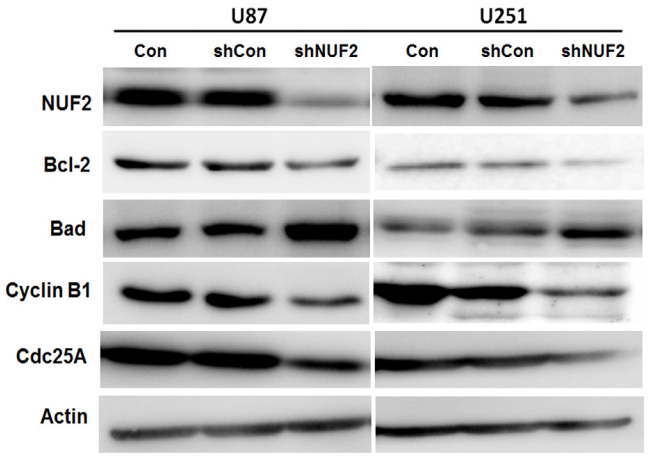

Figure 7. Depletion of NUF2 affects apoptosis-related and G2/M phase-related protein expressions. Ablation of NUF2 caused corresponding decreased expression of apoptosis inhibitor Bcl-2 and increased expression of apoptosis inducer Bad. In addition, depletion of NUF2 in U87 and U251 cells resulted in significant decreases of G2/M phase-related Cyclin B1 and Cdc25A.

Bad induces apoptosis (19, 20). We found that ablation of NUF2 caused corresponding decreased expression of Bcl-2 and increased expression of Bad, confirming that depletion of NUF2 induces apoptosis. Further, depletion of NUF2 in U87 and U251 cells resulted in significant decreases of Cyclin B1 and Cdc25A, which are closely associated with G2/M phase (21, 22). All these data reinforce the notion that depletion of NUF2 affects apoptosis and G2/M phase.

Discussion

Despite current advances in the glioma treatment strategies, the overall survival rate of patients suffering from glioma remains poor. Additionally, currently standard clinic cares for glioma patients, like maximal resection, chemotherapies and/or radiotherapy, have unfortunately resulted in many side effects (23, 24). Currently, cell growth is one of the great burdens and bottleneck of glioma treatments (25). In our study, we investigated the expression profile of NUF2 in human glioma tissues and a range of glioma cell lines. Thereafter, we employed shRNA interference technology to deplete NUF2 expression *in vitro*. Based on the successful construction of lentivirus-delivered shRNA against NUF2, we then assessed the role of NUF2 depletion in glioma growth *in vitro* and *in vivo*.

Consistent with other reports (15), NUF2 was observed to be overexpressed in glioma tissues. However, in a series of glioma cell lines, NUF2 exhibited differentially expression levels (Figure 2). U87 and U251 showed the highest NUF2 expression level, making these two cell lines optimal cell models for subsequent construction of lentivirus that stably depleted NUF2 expression. By infecting U87 and U251 cells with Lv-shNUF2, we found that cell growth was significantly inhibited *in vitro* (Figure 4) and *in vivo* (Figure 5), indicating the robust promotion-effect of NUF2 in glioma tumor growth. Moreover, annexin-V/ PI and cell cycle analysis revealed that depletion of NUF2 induced apoptosis and affected cell proportion in G2/M phase (Figure 6), indicating that regulation of NUF2 could affect G2/M phase and induce eventual cell apoptosis. This notion was consistent with a previous report that depletion of NUF2 resulted in a strong block of prometaphase in cell cycle (11). And it was further reinforced by the observations that apoptosis inducer Bad was upregulated, while pro-apoptotic factor Bcl-2 and G2/M phase regulators Cyclin B1 and Cdc25 were downregulated in response to NUF2 ablation in both U87 and U251 cells (Figure 7). In all, it could be concluded that depletion of NUF2 possibly inhibited glioma cell growth through affecting G2/M phase and eventually leading to cell apoptosis.

Chromosome segregation in mitosis is orchestrated by dynamic interactions between spindle microtubules and the kinetochore, a multiprotein complex assembled onto centromeric DNA of the chromosome (26). In eukaryotes, kinetochore provides a chromosomal attachment point for the mitotic spindle, orienting the chromosome to the microtubule, and functions in initiating, controlling, and monitoring the movements of chromosomes during mitosis. Indeed, human NUF2 was recently reported to interact with centromere-associated protein E and is essential for a stable spindle microtubule-kinetochore attachment (11, 26, 27). In the present study, we provided evidence confirming that NUF2, a key component of NDC80 complex, plays pivotal role in chromosome segregation in mitosis.

The identification of NUF2 as a key molecule involved in glioma cell growth is of significant importance. On one hand, our study indirectly confirmed that NUF2 may be greatly involved in mitosis. From a wider perspective, strict control of NDC80 complex ensures normal mitotic process (especially G2/M phase). However, dysregulation of NDC80 complex may unfortunately lead to cell cycle arrest and even cell death. On the other hand, it is the first report to our knowledge to examine the role of NUF2 in glioma development. Previous reports have focused on the role of NUF2 in non-small cell lung cancer, cervical cancer and colorectal and gastric cancers cell proliferation. Our report may provide evidence that NUF2 is also closely linked with glioma development. And hence, NUF2 is possibly widely involved in human cancer developments.

In all, our results indicate that inhibition of NUF2 expression can exhibit potent antitumor activity. The identification of NUF2 as a key mediator of glioma cell growth could at least provide a novel clue for development of molecular target therapy against glioma.

References

1. Jones D.S., Podolsky S.H., and Greene J.A., The burden of disease and the changing task of medicine. *N. Engl. J. Med.* 2012, **366**: 2333-2338. doi: 10.1056/NEJMp1113569

2. Zhang F., Liu B., Wang Z., Yu X.J., Ni Q.X., Yang W.T., Mukaida N., and Li Y.Y., A novel regulatory mechanism of Pim-3 kinase stability and its involvement in pancreatic cancer progression. *Mol. Cancer Res.* 2013. doi: 10.1158/1541-7786

3. Bhatt A.N., Mathur R., Farooque A., Verma A., and Dwarakanath B.S., Cancer biomarkers - current perspectives. *Indian J. Med. Res.* 2010, **132**: 129-149.

4. Cho W.C., Contribution of oncoproteomics to cancer biomarker discovery. *Mol. Cancer* 2007, **6**: 25. doi: 10.1186/1476-4598-6-25

5. Meyer M.A., Malignant gliomas in adults. *N. Engl. J. Med.* 2008, **359**:492-507. doi: 10.1056/NEJMra0708126 .

6. Louis D.N., Ohgaki H., Wiestler O.D., Cavenee W.K., Burger

P.C., Jouvet A., Scheithauer B.W., and Kleihues P., The 2007 WHO classification of tumours of the central nervous system. *Acta Neuropathol*. 2007, **114**: 97-109. doi: 10.1007/s00401-007-0243-4

7. Anton K., Baehring J.M., and Mayer T., Glioblastoma multiforme: overview of current treatment and future perspectives. *Hematol. Oncol. Clin. North Am.* 2012, **26**: 825-853. doi: 10.1016/j.hoc.2012.04.006

8. Chang L., Su J., Jia X., and Ren H., Treating malignant glioma in Chinese patients: update on temozolomide. *Onco. Targets Ther.* 2014, **7**: 235-244. doi: 10.2147/OTT.S41336

9. Cheerambathur D.K., Gassmann R., Cook B., Oegema K., and Desai A., Crosstalk between microtubule attachment complexes ensures accurate chromosome segregation. *Science* 2013, **342**: 1239-1242. doi: 10.1126/science.1246232

10. He X., Rines D.R., Espelin C.W., and Sorger P.K., Molecular analysis of kinetochore-microtubule attachment in budding yeast. *Cell* 2001, **106**: 195-206.

11. DeLuca J.G., Moree B., Hickey J.M., Kilmartin J.V., and Salmon E.D., hNuf2 inhibition blocks stable kinetochore-microtubule attachment and induces mitotic cell death in HeLa cells. *J. Cell Biol.* 2002, **159**: 549-555.

12. Martin-Lluesma S., Stucke V.M., and Nigg E.A., Role of Hec1 in spindle checkpoint signaling and kinetochore recruitment of Mad1/Mad2. *Science* 2002, **297**: 2267-2270.

13. Hayama S., Daigo Y., Kato T., Ishikawa N., Yamabuki T., Miyamoto M., Ito T., Tsuchiya E., Kondo S., and Nakamura Y., Activation of CDCA1-KNTC2, members of centromere protein complex, involved in pulmonary carcinogenesis. *Cancer Res.* 2006, **66**: 10339-10348.

14. Numnum T.M., Makhija S., Lu B., Wang M., Rivera A., Stoff-Khalili M., Alvarez R.D., Zhu Z.B., and Curiel D.T., Improved antitumor therapy based upon infectivity-enhanced adenoviral delivery of RNA interference in ovarian carcinoma cell lines. *Gynecol. Oncol.* 2008, **108**: 34-41.

15. Kaneko N., Miura K., Gu Z., Karasawa H., Ohnuma S., Sasaki H., Tsukamoto N., Yokoyama S., Yamamura A., Nagase H., Shibata C., Sasaki I., and Horii A., siRNA-mediated knockdown against CDCA1 and KNTC2, both frequently overexpressed in colorectal and gastric cancers, suppresses cell proliferation and induces apoptosis. *Biochem. Biophys. Res. Commun.* 2009, **390**: 1235-1240. doi: 10.1016/j.bbrc.2009.10.127

16. Sakoda T., Kasahara N., Hamamori Y., and Kedes L., A high-titer lentiviral production system mediates efficient transduction of differentiated cells including beating cardiac myocytes. *J. Mol. Cell Cardiol.* 1999, **31**: 2037-2047.

17. Soneoka Y., Cannon P.M., Ramsdale E.E., Griffiths J.C., Romano G., Kingsman S.M., and Kingsman A.J., A transient three-plasmid expression system for the production of high titer retroviral vectors. *Nucleic. Acids Res.* 1995, **23**: 628-633.

18. Zhou J., Xu T., Yan Y., Qin R., Wang H., Zhang X., Huang Y., Wang Y., Lu Y., Fu D., and Chen J., MicroRNA-326 functions as a tumor suppressor in glioma by targeting the Nin one binding protein (NOB1). *PLoS One* 2013, **8**: e68469. doi: 10.1371/journal.pone.0068469

19. Michels J., Kepp O., Senovilla L., Lissa D., Castedo M., Kroemer G., and Galluzzi L., Functions of BCL-X L at the Interface between Cell Death and Metabolism. *Int. J. Cell Biol.* 2013, **2013**: 705294. doi: 10.1155/2013/705294

20. Voellger B., Kirches E., Wilisch-Neumann A., Weise A., Tapia-Perez J.H., Rupa R., Mawrin C., and Firsching R., Resveratrol decreases B-cell lymphoma-2 expression and viability in GH3 pituitary adenoma cells of the rat. *Onco. Targets Ther.* 2013, **9**: 1269-1276. doi: 10.2147/OTT.S45154. eCollection 2013

21. King R.W., Jackson P.K., and Kirschner M.W., Mitosis in transition. *Cell* 1994, **79**: 563-571.

22. Knoblich J.A., and Lehner C.F., Synergistic action of Drosophila cyclins A and B during the G2-M transition. *Embo. J.* 1993, **12**: 65-74.

23. Arko L., Katsyv I., Park G.E., Luan W.P., and Park J.K., Experimental approaches for the treatment of malignant gliomas. *Pharmacol. Ther.* 2010, **128**: 1-36.

24. Mrugala M.M., Advances and challenges in the treatment of glioblastoma: a clinician's perspective. *Discov. Med.* 2013, **15**: 221-230.

25. Li X.Q., Ouyang Z.G., Zhang S.H., Liu H., Shang Y., Li Y., and Zhen Y.S., Synergy of enediyne antibiotic lidamycin and temozolomide in suppressing glioma growth with potentiated apoptosis induction. *J. Neurooncol.* 2014.**119**: 91-100. doi: 10.1007/s11060-014-1477-3

26. Liu D., Ding X., Du J, Cai X., Huang Y., Ward T., Shaw A., Yang Y., Hu R., Jin C., and Yao X., Human NUF2 interacts with centromere-associated protein E and is essential for a stable spindle microtubule-kinetochore attachment. *J. Biol. Chem.* 2007, **282**: 21415-21424.

27. Sundin L.J., Guimaraes G.J., and Deluca J.G., The NDC80 complex proteins Nuf2 and Hec1 make distinct contributions to kinetochore-microtubule attachment in mitosis. *Mol. Biol. Cell* 2011, **22**: 759-768. doi: 10.1091/mbc.E10-08-0671